

Ground-state band in  $^{72}\text{Se}^\dagger$ 

K. P. Lieb\* and J. J. Kolata

Brookhaven National Laboratory, Upton, New York 11973

(Received 23 July 1976)

Yrast states in  $^{72}\text{Se}$  up to  $I^\pi = 14^+$  have been excited in the reaction  $^{58}\text{Ni}(^{16}\text{O}, 2p)$  at 40–58 MeV beam energy. Their mean lifetimes have been determined by using the Doppler shift attenuation method. The measured  $B(E2)$  values of transitions within the ground-state band are discussed in terms of several nuclear models, including the triaxial rotor and interacting boson models. An upper limit of  $\tau_f < 0.1$  ps was deduced for the feeding-time of the highest yrast states.

[ NUCLEAR REACTIONS  $^{58}\text{Ni}(^{16}\text{O}, 2p\gamma)$  40–58 MeV; measured  $E_\gamma$ , relative excitation functions, angular distributions, Doppler shift; deduced  $E_x$ ,  $I^\pi$ ,  $T_{1/2}$ , feeding time. ]

## I. INTRODUCTION

The ground-state band of  $^{72}\text{Se}$  has been the subject of several recent experimental investigations. Nolte *et al.*<sup>1</sup> and Hamilton *et al.*<sup>2</sup> have identified the yrast states up to the  $12^+$  member, using heavy-ion-induced reactions. Properties of some low-spin states have also been established from the  $\beta$  decay of  $^{72}\text{Br}$  (Ref. 3) as well as from a study of the reactions  $^{70}\text{Ge}(\alpha, 2n)$  (Ref. 4) and  $^{58}\text{Ni}(^{16}\text{O}, 2p)$  (Ref. 5). Finally, recoil distance and preliminary Doppler shift attenuation measurements have been reported by various groups.<sup>6,7</sup>

As to the aspect of nuclear structure, the transitional nucleus  $^{72}\text{Se}$  seems to feature a spectrum typical of shape coexistence.<sup>2</sup> This interpretation is based on the rotational-like energy spacings of the yrast states with  $I \geq 6$  and on the occurrence of a low-lying excited  $0^+$  state whose energy fits as band head. Furthermore, the observation of  $K^\pi = \frac{1}{2}^-, \frac{5}{2}^-$  rotational, and  $g_{9/2}$  decoupled bands in the neighboring odd Se and As isotopes<sup>8,9</sup> points to a core deformation of  $\beta = 0.2$ – $0.3$ . On the other hand, considering the quadrupole transitions between the low-spin levels, Löbner *et al.*<sup>7</sup> claim that the anharmonic vibrator model provides a rather consistent description of these states. In particular, this model accounts for the nearly equidistant level spacing up to the  $6^+$  state and the very weak ground-state transition from the second  $2^+$  state.

Of course, measurement of the intrinsic electric quadrupole moment  $Q_0(I)$  of the yrast states would provide the most direct verification of a phase transition between spherical and deformed shapes. Lacking an experimental method to do so, the next best way is to measure electromagnetic

transition probabilities within the ground-state band. We recall that, in the harmonic vibrator model,  $B(E2, I \rightarrow I-2)$  is proportional to the phonon number and therefore to the spin  $I$ , whereas the rigid rotor model with a constant  $Q_0$  predicts a slow increase for this  $B(E2)$  value with increasing spin.<sup>10</sup>

The main object of this study was thus to measure the lifetimes within the ground-state band (gsb) using the Doppler shift attenuation (DSA) method. As previously shown,<sup>6,7</sup> delayed feeding from both discrete states and the “ $\gamma$  continuum” presents serious problems when the levels are excited in heavy-ion-induced fusion evaporation reactions. This point had to be considered very carefully. In particular, the DSA technique should allow us to resolve the discrepancies found in recoil distance measurements<sup>6,7</sup> for the lifetimes of the 1.64-MeV  $4^+$  and 2.47-MeV  $6^+$  states, and attributed to different assumptions for the feeding mechanism. In the course of the experiment, we also identified the probable  $14^+$  member of the gsb and measured its lifetime.

The large number of known (yrast and non-yrast) states and  $E2$  transition probabilities in  $^{72}\text{Se}$  provides a sensitive measure of the shape of this nucleus. In Sec. III, the data will be compared with the predictions of several nuclear models, including the triaxial-rotor model, the interacting-boson model and a simple shape-coexistence model.

## II. EXPERIMENTAL METHODS AND RESULTS

Standard techniques of in-beam  $\gamma$ -ray spectroscopy were employed throughout the experiment, including the measurement of singles  $\gamma$ -ray angular distributions and excitation functions and  $\gamma$ - $\gamma$

coincidences. Since the experimental setup, data storage procedures, and analysis have been communicated previously,<sup>11</sup> we mention here only the details relevant for the DSA measurements.

The experiment was performed using the 100 nA  $^{16}\text{O}^{5+,6+}$  beam of the Brookhaven MP6 tandem accelerator at an energy of 40 to 58 MeV. In this range, the evaporation of two protons from the compound nucleus  $^{74}\text{Kr}$  is the predominant exit channel,<sup>1</sup> leading to states in  $^{72}\text{Se}$ . Other strongly populated evaporation residues<sup>12,13</sup> are  $^{71}\text{As}(3p)$ ,  $^{69}\text{As}(\alpha p)$ , and  $^{68}\text{Ge}(\alpha 2p)$ , for which the emission of charged particles is favored over neutron emission by their respective  $Q$  values.

Isotopically enriched (97.5%)  $^{58}\text{Ni}$  targets 130–580  $\mu\text{g}/\text{cm}^2$  thick were evaporated onto metallic backings of Ag, Au, and Ta in which the beam and the residual nuclei were stopped. In most runs, we used two coaxial Ge(Li) detectors of 15% efficiency having an energy resolution of typically 2.2 keV at 1.33 MeV. They were placed at a distance of 3–5 cm from the target and covered with Fe and Pb absorbers in order to reduce the low energy portion of the spectrum which consisted mainly of x-rays and transitions following Coulomb excitation of the backing.

(1)  $\gamma$ - $\gamma$  coincidences were taken at 52.5-MeV beam energy with the two detectors placed at  $0^\circ$  and  $90^\circ$  to the beam axis. The target was a 580- $\mu\text{g}/\text{cm}^2$  layer of  $^{58}\text{Ni}$  evaporated onto a Ta backing. The data were recorded in the multiparameter mode<sup>14</sup> and stored on magnetic tape. Upon replaying the tapes, gates were set in both detectors on all intense lines. Figure 1 displays a summed coincidence spectrum at  $0^\circ$  obtained with the gates set on the 4–2, 6–4, 8–6, and 10–8 gsb transitions in the  $90^\circ$  spectrum. Coincidences with the 862 keV 2–0 and 1205 keV 12–10 transitions were not included in the sum, since both lines

are degenerate with transitions in  $^{69}\text{As}$  (Refs. 1, 5, and 13). As to the line shapes, it is interesting to note that the lower transitions up to the  $6^+$  state do not show any Doppler broadening, whereas the 8–6 and 10–8 transitions feature both shifted and unshifted components. The line shape of the 12–10 transition, given in the inset of Fig. 1, clearly does not contain any unshifted component which would overlap in the  $\gamma$  singles spectrum with the long lived 1204.5-keV line in  $^{69}\text{As}$  (Ref. 13). This fact justified the DSA analysis of the 12–10 transition in the singles spectra. In coincidence with all gsb transitions, we identified an additional strongly Doppler-broadened line at  $1328.4 \pm 0.5$  keV which we placed on top of the cascade. Its energy, lifetime, and angular distribution (see below) fit well into the trend of the other members of the yrast band, suggesting a stretched  $E2$  transition leading to a probable spin-parity assignment of  $I^\pi = 14^+$  for the 7037-keV state. The coincidence data also confirmed two transitions of 1535 and 1303 keV observed by Bohn *et al.* and attributed to the decays of states at 3172 and 3770 keV, respectively.<sup>15</sup>

(2) *Excitation functions* were measured to determine the minimum energy at which a particular state is strongly enough excited so that its line shape can be clearly distinguished, but is least disturbed by delayed feeding from the next higher state in the band. Also, the amount of side feeding of the 1.64-MeV  $4^+$  and 2.47-MeV  $6^+$  states was obtained in this manner.  $\gamma$  spectra were taken at oxygen energies of 40, 42, 44, 47, 50, 52.5, 55, and 58 MeV. As mentioned before, the 12–10 transition is contaminated by the 1204.5-keV line in  $^{69}\text{As}$ . However, with the Ge(Li) detector positioned at  $0^\circ$  the doublet was fully resolved. In general, the spectra contained sufficient events to allow extraction of the Doppler shifted centroids.

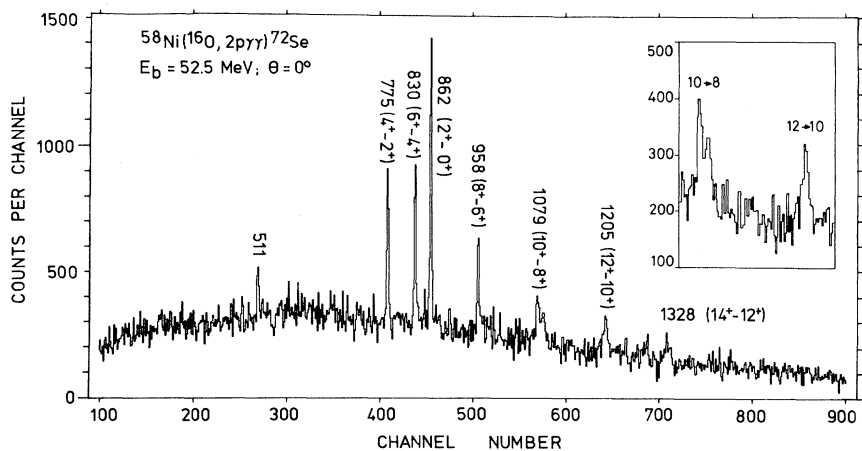


FIG. 1. Summed  $\gamma$ - $\gamma$  coincidence spectrum of the  $0^\circ$  detector with gates set on the 775-, 830-, 958-, and 1079-keV transitions in the  $90^\circ$  detector. The inset shows in more detail the line shapes of the 1079- and 1205-keV transitions.

TABLE I. Energies and angular distributions of transitions in  $^{72}\text{Se}$ .

$E_\gamma$ (keV)	$E_i$ (keV)	$I_i^{\pi_i}$	$E_f$ (keV)	$I_f^{\pi_f}$	$A_2^a$	$A_4$	$\alpha_2^b$
861.9(1)	862	2*	0	0*	+0.151(11)	-0.054(14)	0.21(2) <sup>c</sup>
774.5(1)	1636	4*	862	2*	+0.316(10)	-0.116(14)	0.62(2)
829.9(1)	2466	6*	1636	4*	+0.302(15)	-0.079(21)	0.66(3)
957.8(1)	3424	8*	2466	6*	+0.259(44)	-0.135(60)	0.60(10)
1079.4(2)	4504	10*	3424	8*	...	...	...
1205.4(2)	5709	(12*)	4504	10*	+0.55(12)	-0.14(10)	1.36(20) <sup>d</sup>
1328.4(5)	7037	(14*)	5709	(12*)	+0.49(11)	-0.16(8)	1.22(24)
1303.3(5)	3770		2466	6*	-0.268(35)	0	...
1316.5(2)	1317	2*	0	0*	+0.122(54)	0	0.17(8)
379.8(2)	1317	2*	937	0*	...	...	...
454.7(2)	1317	2*	862	2*	...	...	...
1535.5(2)	3172		1636	4*	...	...	...

<sup>a</sup> Measured at 52.5 MeV beam energy.<sup>b</sup>  $\alpha_2 = A_2/A_2^{\max}$  (see Ref. 16).<sup>c</sup> Obscured by a 863-keV transition in  $^{69}\text{As}$ .<sup>d</sup> Obscured by a 1205-keV transition in  $^{69}\text{As}$ .

(3) *Angular distributions* were recorded at 52.5 MeV with one detector moving in  $10^\circ$  steps between  $15^\circ$  and  $165^\circ$  and the other detector serving as monitor. The coefficients of the terms of Legendre polynomials are listed in Table I. The strong

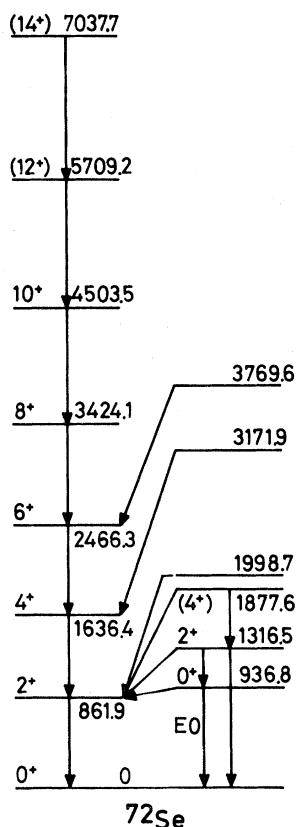


FIG. 2. Proposed partial level scheme of  $^{72}\text{Se}$  as seen in the present work. A similar scheme could also be deduced from results presented in Refs. 5, 7, and 15.

anisotropies of the 7.04 → 5.71- and 5.71 → 4.50-MeV transitions point to a high initial alignment of these states. Assuming  $I^\pi(7.04) = 14^+$  and  $I^\pi(5.17) = 12^+$ , one finds alignment parameters of  $\alpha_2 = 1.22 \pm 0.24$  and  $\alpha_2 = 1.36 \pm 0.20$ , respectively, in the notation of Yamazaki.<sup>16</sup>

The information obtained from analyses of the  $\gamma$  singles and coincidence spectra is listed in Table I. The proposed level scheme shown in Fig. 2 also contains some results of previous studies.<sup>5,7,15</sup>

(4) *Doppler shift attenuation* analyses were performed for the  $0^\circ$   $\gamma$  singles and coincidence spectra. The mean lifetime was deduced from the  $0^\circ/90^\circ$  centroid shift  $\langle \Delta E \rangle$ ,

$$\langle \Delta E \rangle = FE_{\gamma 0} \langle v_z/c \rangle = F \langle \Delta E_{\text{FDS}} \rangle,$$

where  $E_{\gamma 0}$  denotes the unshifted  $\gamma$ -ray energy and  $\langle v_z/c \rangle$  the projection of the recoil velocity along the beam axis averaged over the kinematical spread of the recoiling nuclei and the solid angle of the detector. The full Doppler shift  $\langle \Delta E_{\text{FDS}} \rangle$  was determined experimentally at 47-, 50-, and 52.5-MeV beam energy using a  $450\text{-}\mu\text{g}/\text{cm}^2$  self-supporting foil of natural Ni. At 50 MeV, the strong 775-keV  $4^+ \rightarrow 2^+$  transition exhibits a FDS of  $\langle \Delta E_{\text{FDS}} \rangle = 11.9 \pm 0.1$  keV, corresponding to  $\langle v_z/c \rangle = (1.52 \pm 0.02)\%$ . Due to the small kinematical spread in the recoil energy and angle connected with the evaporation of two nucleons from the compound system,<sup>17</sup> the FDS line shape is quite narrow as illustrated in Fig. 3(d). Lifetimes were evaluated from the attenuation factors  $F$  by using a program<sup>18</sup> which treats nuclear stopping in the approximation of Blaugrund<sup>19</sup> and accounts also for the finite target thickness. Table II contains a summary of the previous<sup>6,7,13</sup> and present lifetime measurements, a detailed discussion of which is given below. The errors quoted for our

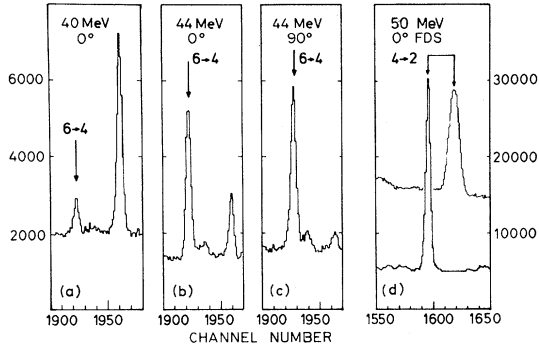


FIG. 3. (a–c). Line shape of the 830-keV  $6^+ \rightarrow 4^+$  transition at 40 and 44 MeV. Note the absence of Doppler broadening. (d) Full Doppler shift of the 775-keV  $4^+ \rightarrow 2^+$  transition at 50-MeV beam energy (both shifted and unshifted transitions are shown).

DSA lifetimes include a 25% contribution due to the uncertainty of the stopping power.

Particular care was taken to discern any Doppler broadening of the 830-keV  $6^+ \rightarrow 4^+$  line which was to be expected from the limit  $\tau(2.47) \leq 0.7$  ps found in a recoil distance (RD) experiment.<sup>7</sup> The  $0^\circ$  line shapes of this transition at 40 and 44 MeV are illustrated in Fig. 3. At 40 MeV, the line profile has a steep right-hand edge and does not show any high energy tail. Similarly, the  $0^\circ$  and  $90^\circ$  line shapes at 44 MeV are nearly identical, indicating that the little peak on the right-hand side is *not* due to Doppler broadening. If we take into account 25% cascade feeding from the 0.8-ps  $8^+$  state and a 20% side feeding from the long-lived 3.77-MeV state,<sup>13</sup> we still expect an observable centroid shift of  $\langle \Delta E \rangle \geq 1.5$  keV and a high energy tail. The limit  $\tau \geq 1.4$  ps deduced from the measured shift  $\langle \Delta E \rangle \leq 1.0$  keV disagrees with

Ref. 7, but is consistent with DSA and RD measurements of the Oak Ridge group<sup>6</sup> as well as with a recent RD experiment by Uhrmacher, Rascher, and Hellmeister.<sup>13</sup> We were not able to resolve a similar discrepancy reported for the lifetime of the 1.64-MeV state,<sup>6,7</sup> as the present experiment gives  $\tau > 1.2$  ps in agreement with all previous data. On the basis of the RD measurement of Ref. 13, a mean life of  $\tau(1.64) = 3.6 \pm 0.8$  ps has been adopted. However, the large variation in reported lifetimes for this state (Table II) suggests the need for yet another measurement. The lifetimes of the 3.42-MeV  $8^+$  and 5.71-MeV  $12^+$  states have been determined at 44 and 47 MeV, respectively, where the corrections due to cascade feeding are small. The lifetimes of the 4.50-MeV  $10^+$  and 7.04-MeV ( $14^+$ ) states, on the other hand, were evaluated from the 52.5-MeV coincidence spectrum, since both line shapes are not fully separated from neighboring transitions in the singles spectra. Figure 4 illustrates the measured centroid shifts of these transitions and the  $F(\tau)$  curves for both runs.

(5) *The feeding time* associated with unobserved transitions preceding the discrete yrast cascade has been estimated from the variation of the apparent lifetime of the 5.71-MeV  $12^+$  state with beam energy. As the average angular momentum deposited in  $^{72}\text{Se}$  increases, a higher  $\gamma$  multiplicity is required to carry it away. This is reflected in the population of states with higher spins as well as in the larger number of  $\gamma$  rays feeding a given yrast state.<sup>20,21</sup> The centroid of the 5709–4504-keV  $12^+ - 10^+$  transition has been evaluated in all  $0^\circ$  spectra between 47 and 58 MeV. The  $F(\tau)$  values presented in Fig. 4 do indeed show a systematic decrease for increasing beam

TABLE II. Summary on mean lives (in ps) in  $^{72}\text{Se}$ : RD, recoil distance technique; DSA, Doppler shift attenuation method.

State		BNL/Köln <sup>a</sup>		München <sup>b</sup>	ORNL/Vanderbilt <sup>c</sup>		Leningrad <sup>d</sup>	Adopted value
$E_x$ (keV)	$I^\pi$							
862	$2^+$	$5.2 \pm 0.6$	RD	$3.6 \pm 0.6$	RD	$5.7 \pm 1.2$	RD	$4.8 \pm 0.5$
1636	$4^+$	$2.7 \pm 0.3$	RD	$1.2 \pm 0.3$	RD	$4.5^{+1.5}_{-1.0}$	RD	$(3.6 \pm 0.8)$
		$>1.2$	DSA			$>2.5$	DSA	
2466	$6^+$	$2.2 \pm 0.2$	RD	$\leq 0.7$	RD	$6.1 \pm 2.5$	RD	$2.4 \pm 0.2$
		$\geq 1.4$	DSA			$2.6 \pm 0.2$	DSA	
3424	$8^+$	$0.90 \pm 0.25$	DSA			$0.75 \pm 0.09$	DSA	$0.80 \pm 0.10$
4504	$10^+$	$0.40 \pm 0.12$	DSA			$0.35 \pm 0.07$	DSA	$0.37 \pm 0.05$
5709	( $12^+$ )	$0.16 \pm 0.04$	DSA			$0.25 \pm 0.04$	DSA	$0.20 \pm 0.04$
7037	( $14^+$ )	$0.08 \pm 0.03$	DSA					$0.08 \pm 0.03$

<sup>a</sup> DSA from present work, RD from Ref. 13.

<sup>b</sup> Reference 7.

<sup>c</sup> Reference 6.

<sup>d</sup> I. M. Lemberg, quoted in Ref. 6.

<sup>e</sup> Not corrected for feeding.

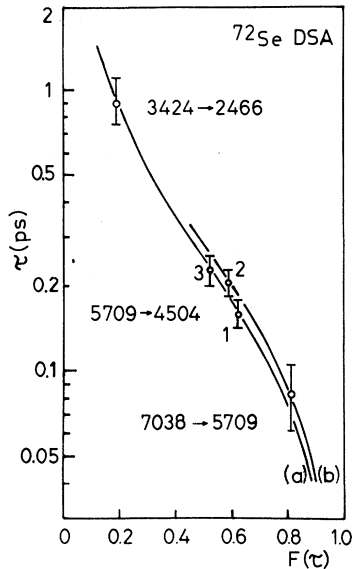


FIG. 4. Measured  $F(\tau)$  values and calculated  $F(\tau)$  curves for (a)  $130 \mu\text{g}/\text{cm}^2$   $^{58}\text{Ni}$  target on Au backing, (b)  $580 \mu\text{g}/\text{cm}^2$   $^{58}\text{Ni}$  target on Ta backing. The different  $F(\tau)$  values for the 5709  $\rightarrow$  4504-keV transition are discussed in the text.

energy; point 1 corresponds to the measurement at 47 MeV and is considered to be unperturbed by feeding; point 2 was taken from the 52.5-MeV coincidence spectrum, whereas point 3 represents the average of the 52.5-, 55-, and 58-MeV singles data. The variation of the observed lifetime from  $\tau = 0.16 \pm 0.02$  ps to  $\tau = 0.24 \pm 0.02$  ps is partly due to the increasing population of the 7.04-MeV state. (Since the two numbers were obtained from the same target/backing, only statistical errors are quoted.) After correcting for the finite lifetime of the 7.04-MeV level, there still remains a time difference of  $0.05 \pm 0.03$  ps which one may tentatively associate with the feeding time of the  $12^+$  and/or  $14^+$  level.

This interpretation is of course not unambiguous, as the expected lifetime of the  $16^+$  member of the gsb has the same magnitude. If this state is contributing to the population of the  $(14^+)$  state, the feeding time could be much shorter. If, on the other hand, we make the most unfavorable assumption that the observed lifetime  $\tau = 0.08 \pm 0.04$  ps of the 7.04-MeV state is mostly due to feeding and that its "true" lifetime is much shorter, we still arrive at an upper limit of  $\tau_f < 0.1$  ps for the feeding time. However, this latter assumption appears to be very unrealistic, since  $\tau(7.04) < 0.05$  ps corresponds to more than 200 Weisskopf units for the  $14^+ \rightarrow 12^+$   $E2$  transition.

### III. DISCUSSION

#### A. Feeding time

We define feeding as the delayed population of a level via unobserved discrete or continuum  $\gamma$ -ray transitions. From the point of view of the measurement of nuclear lifetimes, the feeding time  $\tau_f$  constitutes the limit to which such measurements are feasible in singles experiments. So far, very few experiments have been performed to determine  $\tau_f$ . In oxygen- and neon-induced fusion-evaporation reactions on heavy targets,<sup>21</sup> feeding times up to 30 ps have been encountered. It has been concluded that, in this mass region, no reliable lifetime measurements are possible in even-even nuclei except for the lowest yrast states.

In lighter systems, however, the picture is more encouraging. Sarantites, Barker, and Lu<sup>20</sup> investigated feeding times for three low-lying states in  $^{61}\text{Cu}$  ( $I^\pi = \frac{3}{2}^-, \frac{1}{2}^-$ ;  $\tau \sim 0.5$  ps) populated in the reaction  $^{58}\text{Ni}(\alpha, p)$  at 19.7-MeV beam energy. By measuring Doppler-broadened line shapes in coincidence with protons leading to different excitation energies  $E_x$  in  $^{61}\text{Cu}$ , they observed a linear increase of the effective lifetime with  $E_x$  and deduced an average feeding time of  $\tau_f = 0.3$  ps, if the  $\gamma$  deexcitation starts at the most strongly excited region at  $E_x = 9.5$  MeV.

Halbert *et al.*<sup>22</sup> recently measured lifetimes and  $\gamma$  multiplicities within the gsb of  $^{74}\text{Se}$  using the reaction  $^{64}\text{Ni}(^{16}\text{O}, \alpha 2n)^{74}\text{Se}$ . At 67- and 81-MeV bombarding energies, the average  $\gamma$  multiplicity was found to be  $\langle M \rangle = 9.3$  and 12, respectively.

For the mean life of the 8.12-MeV  $16^+$  state, which was the highest yrast state observed, these authors obtained  $\tau = 0.17 \pm 0.04$  ps (which number includes the "true" lifetimes of the  $16^+$  and  $18^+$  states and the feeding time). By assuming  $\tau(16^+) \approx \tau(18^+) \approx 0.05$  ps, a feeding time of  $\tau_f \sim 0.07$  ps was obtained.

Our measurement for the  $12^+$  and  $14^+$  states in  $^{72}\text{Se}$  parallels the situation in  $^{74}\text{Se}$  in many respects. In particular, preliminary statistical model calculations<sup>23</sup> indicate that the energy and angular momentum matching conditions are very similar to those in  $^{74}\text{Se}$ . The limit  $\tau_f < 0.1$  ps in both nuclei suggests that oxygen-induced reactions in this mass region are suitable for measuring nuclear lifetimes as low as 0.5 ps without corrections for feeding-time effects.

#### B. Nuclear model calculations

Including the present results, a total of 11  $E2$  transition strengths within the gsb and from the decay of the 937-keV  $0_2^+$  and 1317-keV  $2_2^+$  states are known. In addition, relative  $E2$  strengths<sup>3</sup> from the decay of the 1876-keV ( $4_2^+$ ) state can be

TABLE III. Electric quadrupole transition probabilities in  $^{72}\text{Se}$ .

Transition	Experiment	Harmonic vibrator <sup>a</sup>	Soft asymm. rotor <sup>b</sup>	Interacting-boson model		Coexistence model	
				IB <sup>0</sup> <sup>c</sup>	IB <sup>1</sup> <sup>d</sup>	e	f
$B(E2)$ value ( $10^{-2} e^2 b^2$ )							
$2_1 \rightarrow 0_1$	$3.6 \pm 0.4$	$3.2 \pm 0.2$	$3.2 \pm 0.3$	4.2	3.6	$3.6 \pm 0.4$	3.2
$4_1 \rightarrow 2_1$	$(8.2 \pm 1.8)$	$6.4 \pm 0.4$	$5.7 \pm 0.5$	7.7	7.4	$6.3 \pm 0.9$	8.7
$6_1 \rightarrow 4_1$	$8.1 \pm 0.7$	$9.6 \pm 0.6$	$9.2 \pm 0.9$	10.6	11.3	$13.8 \pm 1.9$	12.9
$8_1 \rightarrow 6_1$	$12.7 \pm 1.6$	$12.8 \pm 0.8$	$12.2 \pm 1.3$	12.7	15.0	$14.4 \pm 2.1$	
$10_1 \rightarrow 8_1$	$15.1^{+2.4}_{-1.8}$	$16.0 \pm 1.0$	$15.1 \pm 1.5$	14.1	18.6	$14.8 \pm 2.1$	
$12_1 \rightarrow 10_1$	$16.0^{+4.0}_{-2.7}$	$19.2 \pm 1.2$	$18.0 \pm 1.8$	14.9		$15.1 \pm 2.2$	
$14_1 \rightarrow 12_1$	$24.7^{+14.8}_{-6.7}$	$22.4 \pm 1.4$	$20.9 \pm 2.1$	14.9		$15.2 \pm 2.2$	
$0_2 \rightarrow 2_1$	$28.0 \pm 5.2^g$	$6.4 \pm 0.4$	$4.4 \pm 0.5$	7.7	8.2	$21.9 \pm 2.1$	14.6
$2_2 \rightarrow 0_1$	$0.084 \pm 0.018$	0	$0.08 \pm 0.02$	0	0.08	$3.6 \pm 0.4$	
$2_2 \rightarrow 0_2$	$8.7 \pm 2.3^g$	0		8.7	4.1	$4.4 \pm 0.6$	
$2_2 \rightarrow 2_1$	$12.9 \pm 2.8^g$	$6.4 \pm 0.4$	$4.5 \pm 0.5$	7.7	4.5	$3.1 \pm 0.4$	
Quadrupole moment $Q(2_1)$ (eb)							
	$(-0.32 \pm 0.05)^h$	0	$-0.40 \pm 0.05$	$-0.56$		$-0.30 \pm 0.02$	

<sup>a</sup> $B(E2, 2_1 \rightarrow 0_1) = 320 \pm 20 e^2 \text{ fm}^4$  from fit to yrast transitions.

<sup>b</sup>Parameters are  $Q_0 = 1.14 \pm 0.07 \text{ eb}$ ,  $\gamma = 27^\circ$ ,  $\mu = 0.6$ .

<sup>c</sup>IB<sup>0</sup> parameters are  $N = 12$ ,  $q_2 = 0.205 \text{ eb}$ ,  $q'_2 = 0.33 \text{ eb}$ .

<sup>d</sup>IB<sup>1</sup> parameters are  $N = 12$ ,  $q_2 = 0.174 \text{ eb}$ ,  $q'_2 = 0.118 \text{ eb}$ ,  $\xi = 0.10$ ,  $\xi' = 0.27$ .

<sup>e</sup>See text.

<sup>f</sup>Reference 6.

<sup>g</sup>References 2, 3, and 7;  $E2/M1$  mixing ratio of  $2_2 \rightarrow 2_1$  transition from Ref. 5.

<sup>h</sup>Average value of  $Q(2_1)$  in  $^{76,78,80}\text{Se}$  (Ref. 32).

obtained from the measured branching ratios. With this large number of  $B(E2)$  values summarized in Table III,  $^{72}\text{Se}$  constitutes an exceptionally good and interesting case for testing nuclear model calculations.

In the following section, we first discuss the two limiting models of rigid or soft rotation and harmonic quadrupole surface vibrations<sup>24</sup> which already account for some properties of the upper and lower part of the gsb, respectively. The calculations will then be extended to a simple shape-coexistence model proposed by Dietrich<sup>25</sup> for the light mercury isotopes and an interacting-boson model (in the vibrational limit) discussed by Janssen, Jolos, and Dönau<sup>26</sup> and by Arima and Iachello.<sup>27</sup> A comparison with the gsb energies and  $E2$  transitions in  $^{74}\text{Se}$  recently studied by Halbert *et al.*<sup>22</sup> will further clarify the collective behavior of the even Se isotopes.

### 1. Rotation and harmonic vibration

In Fig. 5, we compare the  $B(E2)$  values and the quantity  $S_I = (E_I - E_{I-2})/(4I - 2)$  for the yrast bands in  $^{72}\text{Se}$  and  $^{74}\text{Se}$  with the predictions of the rotational and vibrational models. In the limit of a symmetric rotor with a constant moment of inertia  $\theta$ , one expects  $S_I = \hbar^2/2\theta = \text{const}$ , whereas

$S_I = \hbar \omega_2/(4I - 2)$  in the limit of harmonic vibrations. The gsb in  $^{72}\text{Se}$  follows the vibrational spectrum up to  $I = 6$ . For  $I > 6$ , the  $S_I$  values in  $^{72}\text{Se}$  and  $^{74}\text{Se}$  agree within about 0.8 keV and show a behavior typical of soft triaxial rotation or anharmonic vibration (see below). The  $E2$  matrix elements of the yrast transitions, on the other hand, seem to show different trends in the two nuclei: the  $B(E2)$  values in  $^{72}\text{Se}$  increase by a factor of 6, whereas in  $^{74}\text{Se}$  they seem to stay constant. One should, however, keep in mind that the  $^{74}\text{Se}$  DSA data for  $I > 8$  have not been corrected for feeding and that the corresponding  $B(E2)$  values may be systematically too low.<sup>22</sup>

For a harmonic vibrator, the yrast  $B(E2)$  values increase proportionally to the spin  $I$ .<sup>10</sup> Writing  $B(E2, I \rightarrow I - 2) = B_{\text{vib}} I$ , one obtains  $B_{\text{vib}} = 320 \pm 20 e^2 \text{ fm}^4$  from the fit to the data displayed in Fig. 5. The other  $B(E2)$  values given in Table III may be considered as a test of the model. The  $E2$  strength and the large  $E2/M1$  mixing ratio of the  $2_2^+ \rightarrow 2_1^+$  one phonon transition<sup>5</sup> and the (strictly forbidden)  $2_2 \rightarrow 0_1$  two-phonon transition are quite well accounted for. On the other hand,  $E2$  transitions involving the 937-keV  $0_2^+$  state are not reproduced, the discrepancy being most serious for the  $2_2 \rightarrow 0_2$  transition.

The measured yrast energies and  $E2$  transition probabilities are incompatible with the model of rigid rotation of a symmetric spheroid. From the  $B(E2)$  values of the upper three yrast transitions, an intrinsic quadrupole moment of  $Q_0 = 2.10 \pm 0.14$  eb is deduced, but the lower yrast transitions are systematically weaker than predicted (see Fig. 5).

From an analysis of the decoupled  $g_{9/2}$  proton bands in  $^{71,73}\text{As}$  (Ref. 8), Toki and Faessler<sup>28</sup> concluded that these nuclei have a rather stable triaxial shape with  $\beta = 0.25$ ,  $\gamma \sim 27^\circ$ . It might therefore be more reasonable to consider the rotation of a triaxial spheroid. In the limit  $\gamma = 30^\circ$ , the yrast energies are given by<sup>29</sup>

$$E_{In} = \frac{3\hbar^2}{8\theta} [I(I+4) + 3n(2I-n)], \quad (1)$$

where  $n \geq 0$  is the so-called wobbling number<sup>24</sup> ( $I = n, n+2, \dots$ ). The point to be stressed is the presence of a linear term in  $I$  which, however, for  $n=0$  (gsb) is much smaller than observed experimentally. At the same time, the yrast  $B(E2)$  values follow the pattern of the symmetric rotor and are in disagreement with the data. We therefore conclude that the gsb in  $^{72}\text{Se}$  cannot be explained by the rigid rotor model. This is in con-

trast to the odd isotopes  $^{73,75}\text{Se}$  (Ref. 9), where the  $K = \frac{5}{2}^-$  [303] bands show a fairly regular  $I(I+1)$  level ordering up to  $I = \frac{17}{2}$ .

A better fit is achieved if a soft rotor coupling to surface vibrations is considered, as proposed by Davydov and collaborators.<sup>30</sup> In this model, the  $E2$  matrix elements depend on  $Q_0$ ,  $\gamma$ , and the parameter  $\mu$  that characterizes nuclear deformability with respect to  $\beta$  vibrations. The yrast  $B(E2)$  values suggest the parameters  $\gamma = (27 \pm 2)^\circ$ ,  $\mu \approx 0.6$ , and  $Q_0 = 1.14 \pm 0.07$  eb corresponding to a deformation of  $\beta = 0.18 \pm 0.02$  and a spectroscopic quadrupole moment of  $Q(2_1) = -0.40 \pm 0.05$  eb. The strong rotational-vibrational coupling is supported by the energy spectrum which becomes phononlike in the limit  $\gamma = 30^\circ$ ,  $\mu = 1$ . Again, the energy and the  $B(E2)$  transition rates of the excited  $0^+$  state are not reproduced in this model (see Table III).

## 2. Shape coexistence

It was first noted by Hamilton *et al.*<sup>2</sup> that the apparent transition from a vibrational to a rotational structure in the gsb of  $^{72}\text{Se}$  is very similar to the one observed in  $^{184,186}\text{Hg}$  (Ref. 31). In these mercury isotopes, the "shape isomerism" has been associated with a second minimum of the

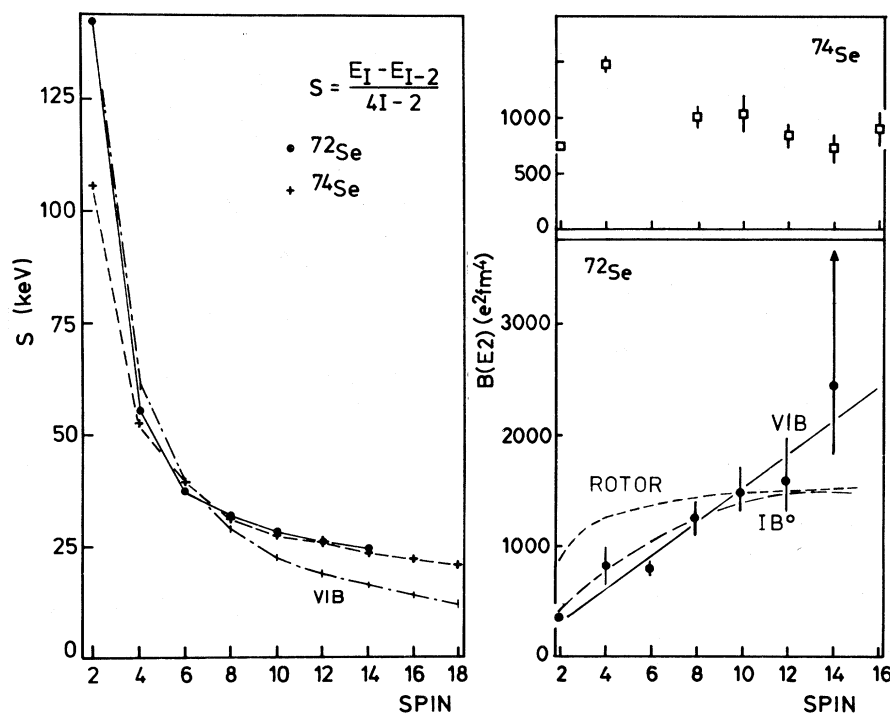


FIG. 5. Energy differences  $S_I$  and  $B(E2)$  values of the yrast cascades in  $^{72}\text{Se}$  and  $^{74}\text{Se}$ . The theoretical  $B(E2)$  values for  $^{72}\text{Se}$  refer to the symmetric rigid rotor (ROTOR), the harmonic vibrator (VIB), and the interacting-boson model ( $\text{IB}^0$ ). The  $B(E2)$  values in  $^{74}\text{Se}$  were taken from Refs. 2 and 37 and have not been corrected for feeding.

potential energy surface at a prolate deformation of  $\beta \approx 0.3$  which competes with a nearly spherical minimum. The crossing of the rotational band with the phonon spectrum occurs at a quite low spin of  $I_{cr} = 2$  or 4. Following Dietrich and Dickmann,<sup>25</sup> one may therefore assume that the two lowest  $2^+$  states mix strongly with each other and that their wave functions can be written as

$$|2_1\rangle = a_2|v_2\rangle + b_2|r_2\rangle,$$

$$|2_2\rangle = b_2|v_2\rangle - a_2|r_2\rangle.$$

Here,  $|v_2\rangle$  and  $|r_2\rangle$  denote the vibrational and rotational  $2^+$  states and the coefficients  $a_2$  and  $b_2$  are normalized to unity. If we assume that the yrast states with  $I > 4$  represent a rotational band built upon the 937-keV  $0_2^+$  state and that their energies are given by

$$E_I = E_0 + \frac{\hbar^2}{2\theta} I(I+1) + bI^2(I+1)^2,$$

we obtain  $E_0 = 937$  keV,  $\hbar^2/2\theta = 36.8 \pm 0.2$  keV, and  $b = -37 \pm 1$  eV, with an average energy deviation of 29 keV. It should be noted that the moment of inertia parameter is considerably smaller than the ones found in the odd Se isotopes<sup>9</sup> which range from 45 to 58 keV.

The  $B(E2)$  values depend on  $a_2$  and  $b_2$ , the intrinsic quadrupole moment ( $Q_0 = 2.10 \pm 0.14$  eb, taken from the highest three yrast transitions), and the  $2 \rightarrow 0$  phonon transition strength  $B_{vib}$ .<sup>2,25</sup> In column 4 of Table III, the measured transition strengths are compared with the predictions of this simple model using the parameters  $a_2 = b_2 = 1/\sqrt{2}$  proposed by Ramayya *et al.*<sup>2</sup> in order to fit the very strong  $0_2 \rightarrow 2_1$  transition. The  $B(E2)$  values of most yrast transitions and the  $2_2 \rightarrow 0_2$  transition are reasonably well reproduced, whereas the  $2_2 \rightarrow 2_1$  transition is underestimated by a factor of 2.5. Although the quadrupole moment of the lowest  $2^+$  state in  $^{72}\text{Se}$  has not been measured, the average value  $Q_2 = -0.32 \pm 0.05$  eb obtained recently<sup>32</sup> for the neighboring isotopes  $^{76,78,80}\text{Se}$  is in good agreement with the predicted value  $Q_2 = -0.30$  eb. Serious disagreement by a factor of 40 is found for the  $2_2 \rightarrow 0_1$  transition, however. This very weak transition can be fitted only if we consider mixing in both the  $0^+$  and  $2^+$  states ( $a_0 = 0.89 \pm 0.05$ ,  $b_0 = -0.45 \pm 0.15$ ,  $a_2 = b_2 = 1/\sqrt{2}$ ) so as to produce destructive interference in the  $2_2 \rightarrow 0_1$ , and constructive interference in the  $0_2 \rightarrow 2_1$  transition. This solution implies, however, that the two potential energy minima are not well separated and it might be artificial to speak of two distinct deformations.

### 3. Interacting-boson (IB) model

We finally discuss  $^{72}\text{Se}$  in terms of the vibrational limit of the interacting-boson model in the version of Arima and Iachello.<sup>27</sup> By exploiting the  $\text{SU}(5) \supset 0^+(5)$  group structure, these authors derived analytical relations for the energies and transition rates. This model, which corresponds to some extent to the anharmonic vibrator, is similar to those proposed by Das, Dreizler, and Klein,<sup>23</sup> Brink, de Toledo-Piza, and Kerman,<sup>34</sup> and Janssen *et al.*<sup>26</sup> There are several experimental indications which motivated this approach:

(1) The strongest hint is the linear dependence on the spin  $I$  of the measured yrast  $\gamma$ -ray energies  $E_I - E_{I-2}$  (for  $I \geq 6$ ), as shown in Fig. 6. This tendency is even more pronounced in  $^{74}\text{Se}$ , where  $\Delta E_I$  closely follows a straight line up to  $I = 18$ . It has been customary<sup>35</sup> to write  $\Delta E_I = \epsilon + \frac{1}{2}c_4(I-2)$ , where  $\epsilon$  is the phonon energy and  $c_4$  the anharmonicity of the lowest  $4^+$  state. Since  $\Delta E_2$  and  $\Delta E_4$  in  $^{72}\text{Se}$  deviate from the linear relationship,  $\epsilon$  and  $c_4$  cannot be taken from the energy of the  $2^+$  and  $4^+$  states, but were fitted from the higher yrast transitions.

(2) As pointed out before,  $A \sim 70$  nuclei seem to have rather stable  $\gamma$  deformation ( $\beta = 0.25$ ,  $\gamma \sim 27^\circ$  for  $^{71,73}\text{As}$ , Ref. 28). Similar deformation parameters have been found, for example in the  $A = 130$  region.<sup>29</sup> The successful application<sup>36</sup> of the IB model to  $^{134}\text{Ba}$  ( $\beta = 0.18$ ,  $\gamma = 27^\circ$ ) motivated us to extend it to  $^{72}\text{Se}$ .

(3) The IB model features a finite phonon num-

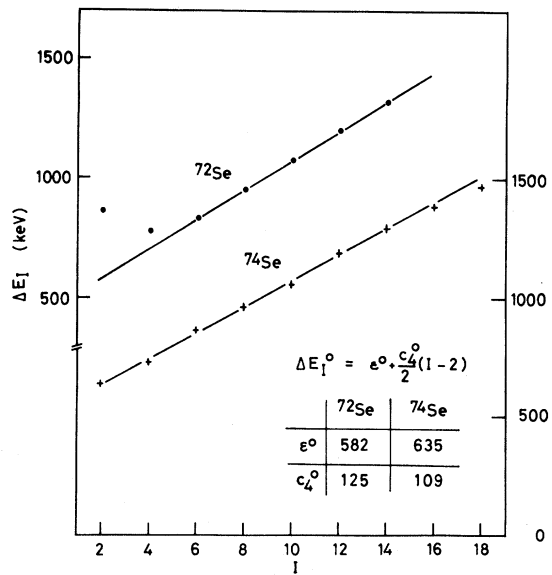


FIG. 6. Fits to the energy differences  $\Delta E_I = E_I - E_{I-2}$  of the gsb in  $^{72,74}\text{Se}$  (IB<sup>0</sup>).



ber  $N$  which strongly affects the  $E2$  transitions between the high spin yrast states. The ratio  $B(E2, I \rightarrow I-2)/B(E2, 2 \rightarrow 0) = (2N+2-I)I/4N$  reaches a maximum for  $I \sim N$ , but affects very little the low-spin transitions. Our data are not inconsistent with such a parabolic pattern for the  $B(E2)$  values with  $N \geq 12$  (see Fig. 5).

The IB calculations were first performed for unbroken  $SU(5)$  symmetry and the results are labelled  $IB^0$  in Figs. 5–7 and Table III. The energy parameters deduced are  $\epsilon^0 = 582 \pm 2$  keV,  $c_4^0 = 124.7 \pm 0.5$  keV in  $^{72}\text{Se}$  (if the ground state and the  $2_1^+$  state are omitted from the fit), and  $\epsilon^0 = 635 \pm 5$  keV,  $c_4^0 = 109 \pm 2$  keV in  $^{74}\text{Se}$ . The yrast energies in  $^{72}\text{Se}$  ( $I \geq 4$ ) are given by

$$E_I^0 = E_0 + \frac{1}{8}(4\epsilon - 3c_4^0)I + \frac{1}{8}c_4^0 I(I+1), \quad (2)$$

where  $E_0 = 347 \pm 3$  keV. This fit, shown in Fig. 7, reproduces the yrast states with  $I \geq 4$  to within 5 keV, which is remarkable for such a light nucleus. On the other hand, if the ground state and the  $2_1^+$  state are included, one obtains  $\epsilon^0 = 731 \pm 48$  keV,  $c_4^0 = 91 \pm 4$  keV, and an average deviation of 53 keV. In the  $IB^0$  model, the  $E2$  matrix elements depend on the phonon cutoff parameter ( $N = 12$ ) and two independent “effective charges”  $q_2$  and  $q_2'$ . They are usually fixed from  $B(E2, 2_1 \rightarrow 0_1) = q_2^2$  and the quadrupole moment  $Q(2_1^+) = -1.52 q_2'$ . Since  $Q(2_1^+)$  has not been measured and the lifetime of the  $2_1^+$  state is still uncertain, we determined  $q_2$

$= 0.205 \pm 0.015$  eb from a fit to all yrast transitions shown in Fig. 5 and  $q_2' = 0.33 \pm 0.04$  eb from the  $2_2^+ \rightarrow 0_2^+$  transition strength. The predicted quadrupole moment  $Q(2_1^+) = -0.56 \pm 0.07$  eb turns out to be about twice the values obtained for  $^{76,78,80}\text{Se}$  (Ref. 32). Except for the forbidden  $2_2 \rightarrow 0_1$  two-phonon transition, all other  $B(E2)$  values depend only on  $q_2$  and are fairly well reproduced.

The nonvanishing  $2_2 \rightarrow 0_1$  transition rate indicates that  $SU(5)$  symmetry is broken to some extent and we therefore investigated this effect. Since the  $2_2 \rightarrow 0_1$  matrix element is small, symmetry breaking due to phonon-number-changing terms in the Hamiltonian may be treated in first order perturbation theory as done in a recent paper by Arima and Iachello.<sup>27</sup> The results of this calculation are labeled  $IB^1$  in Fig. 7 and Table III. The energies and electromagnetic transition rates now depend also on the perturbation parameters  $\xi$  and  $\xi'$ , which were adjusted so as to improve the fit to the energies of the ground state and the  $2_1^+$  state. However, the best fit shown in Fig. 7 ( $\xi = 0.1$ ,  $\xi' = 0.27$ ) only slightly reduces the average energy deviation from 53 keV to 33 keV over the whole yrast cascade. On the other hand, the yrast  $E2$  matrix elements increase faster than observed experimentally. We conclude that, for  $\xi, \xi' \leq 0.4$ , no significant improvement as compared with  $IB^0$  is achieved.

#### IV. CONCLUSION

Doppler shift attenuation analyses of six yrast transitions in  $^{72}\text{Se}$  have been performed in  $0^0 \gamma$  singles and  $\gamma$ - $\gamma$  coincidence spectra. Great care was taken to correctly account for the time delay introduced by the simultaneous population of several members of the gsb and to choose the lowest bombarding energy possible to excite a particular state. Our data are consistent with a feeding time of  $< 0.1$  ps associated with unobserved discrete and statistical  $\gamma$ -ray transitions to the 5.71-MeV  $12^+$  state. For many stretched  $E2$  transitions in this mass region, lifetimes of the order of 0.5 ps have been measured<sup>1,8</sup> in oxygen-induced fusion-evaporation reactions. The present experiment shows that these lifetimes are very little affected by feeding from the continuum and that the conclusions drawn from them concerning nuclear structure are unchanged.

In the gsb of  $^{72}\text{Se}$ , a systematic increase of the  $B(E2)$  values with spin up to  $I = 14$  has been observed, contrary to the trend found in  $^{74}\text{Se}$ . This increase is in disagreement with the picture of rigid rotation of an axially symmetric or triaxial spheroid. Better agreement is obtained by con-

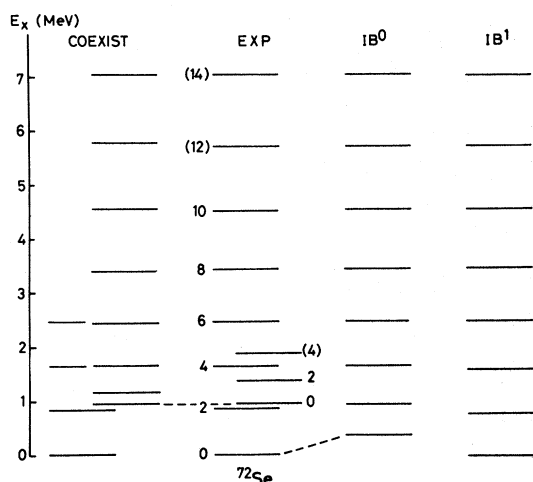


FIG. 7. Comparison of the experimental level scheme of  $^{72}\text{Se}$  with model calculations. For the coexistence model (COEXIST) the rotational band built on the 937-keV  $0_2^+$  state has been parametrized as  $E_I = E_0 + aI(I+1) + bI^2(I+1)^2$ , with  $a = 36.8 \pm 0.2$  keV,  $b = 37 \pm 1$  eV,  $E_0 = 937$  keV. The  $IB^0$  model parameters are  $\epsilon^0 = 582 \pm 2$  keV,  $c_4^0 = 124.8 \pm 0.5$  keV; that of  $IB^1$  are  $\epsilon^1 = 839$  keV,  $c_4^1 = 94.4$  keV,  $\xi = 0.1$ ,  $\xi' = 0.27$ .

sidering a soft triaxial rotor with large rotation-vibration coupling ( $\gamma = 27^\circ$ ,  $\mu = 0.6$ ). The interacting-boson model in the vibrational limit<sup>27</sup> was found to give an excellent fit to the energies of the yrast states ( $4 \leq I \leq 14$ ) and to reproduce, within a factor of 3 or better, all measured  $B(E2)$  values. A more precise measurement of the lifetimes of the upper three yrast levels should allow one to further restrict the phonon cutoff parameter which was set to  $N = 12$  in this analysis, and to check whether the  $B(E2)$  values start decreasing for higher spins as predicted by the model.

In spite of the partial success of the IB model, there still remain difficulties with the interpretation of the very low-lying  $0_2^+$  state and the  $2_1^+$  and  $2_2^+$  states as emphasized by several authors.<sup>2,7,37</sup> If one assumes that a shape transition occurs from

a spherical to a deformed shape, strong mixing between the  $0^+$  states and the  $2^+$  states is required if the five  $E2$  matrix elements connecting these states are to be understood. One promising possibility is to consider a pairing vibration, which in  $N$  or  $Z \approx 38$  nuclei is very, very low in energy.<sup>38</sup>

#### ACKNOWLEDGMENTS

We are indebted to Professor F. Iachello and Dr. J. Meyer-ter-Vehn for illuminating discussions and to Dr. M. Uhrmacher, K. O. Zell, and H. P. Hellmeister for the permission to quote results prior to publication. One of the authors (K.P.L.) acknowledges the hospitality extended to him during a summer fellowship by his colleagues at the Brookhaven National Laboratory.

†Supported in part by U.S.E.R.D.A. and Bundesministerium für Forschung und Technologie.

\*Permanent address: Institut für Kernphysik, Universität zu Köln, Germany.

- <sup>1</sup>E. Nolte, W. Kutschera, Y. Shida, and H. Morinaga, Phys. Lett. **33B**, 294 (1970); E. Nolte, Ph.D. thesis, München, 1973 (unpublished); E. Nolte, Y. Shida, W. Kutschera, R. Prestele, and H. Morinaga, Z. Phys. **A268**, 267 (1974).
- <sup>2</sup>J. H. Hamilton *et al.*, Phys. Rev. Lett. **32**, 239 (1974); A. V. Ramayya *et al.*, Phys. Rev. C **12**, 1360 (1975).
- <sup>3</sup>W. E. Collins, J. H. Hamilton, R. L. Robinson, H. J. Kim, and J. L. C. Ford, Phys. Rev. C **9**, 1457 (1975).
- <sup>4</sup>W. Wyckoff and J. E. Draper, Phys. Rev. C **8**, 796 (1973).
- <sup>5</sup>T. Doron and M. Blann, Nucl. Phys. **A161**, 12 (1971); H. L. Crowell *et al.*, Bull. Am. Phys. Soc. **21**, 188 (1976).
- <sup>6</sup>N. C. Singhal *et al.* in *Reactions between Heavy Nuclei*, edited by R. L. Robinson *et al.* (North-Holland, Amsterdam, 1974), Vol. 1, p. 168; J. H. Hamilton *et al.*, Phys. Rev. Lett. **36**, 340 (1976); I. M. Lemberg *et al.*, in *Abstracts of the Twenty-Fifth Nuclear Structure Conference of the Soviet Academy of Sciences, Leningrad*, 1975 (Academy of Sciences, Moscow, USSR, 1975), p. 376; and private communication from I. M. Lemberg to J. H. Hamilton as quoted by the ORNL/Vanderbilt group.
- <sup>7</sup>K. E. G. Löbner *et al.*, Z. Phys. **A274**, 251 (1975).
- <sup>8</sup>B. Heits *et al.*, Phys. Lett. **61B**, 33 (1976).
- <sup>9</sup>K. O. Zell, H. G. Friederichs, B. Heits, P. von Brentano, and C. Protop, Z. Phys. **A272**, 27 (1975); and (unpublished).
- <sup>10</sup>M. A. Preston, *Physics of the Nucleus* (Addison-Wesley, Reading, Massachusetts, 1962), pp. 333–348.
- <sup>11</sup>J. J. Kolata, P. Gorodetzky, J. W. Olness, A. R. Poletti, and E. K. Warburton, Phys. Rev. C **9**, 953 (1974).
- <sup>12</sup>R. L. Robinson, H. J. Kim, and J. L. C. Ford, Phys. Rev. C **9**, 1402 (1974).
- <sup>13</sup>M. Uhrmacher, R. Rascher, and H. P. Hellmeister

(private communication).

- <sup>14</sup>J. Dauk, Ph.D. thesis, Köln, 1974 (unpublished).
- <sup>15</sup>H. Bohn *et al.*, Jahresbericht, TU München, 1974 (unpublished).
- <sup>16</sup>T. Yamazaki, Nucl. Data **A3**, 1 (1967).
- <sup>17</sup>K. P. Lieb, M. Uhrmacher, J. Dauk, and A. M. Kleinfeld, Nucl. Phys. **A223**, 445 (1974).
- <sup>18</sup>G. A. P. Englebertink and J. W. Olness, Phys. Rev. C **5**, 431 (1972).
- <sup>19</sup>A. E. Blaugrund, Nucl. Phys. **88**, 501 (1966).
- <sup>20</sup>D. G. Sarantites, J. H. Barker, and N. H. Lu, Phys. Rev. C **9**, 603 (1974).
- <sup>21</sup>J. O. Newton, F. S. Stephens, and R. M. Diamond, Nucl. Phys. **A210**, 19 (1973); W. Trautmann, D. Proetel, O. Häusser, W. Hering, and F. Riess, Phys. Rev. Lett. **35**, 1694 (1975).
- <sup>22</sup>M. L. Halbert *et al.*, Nucl. Phys. **A259**, 496 (1976).
- <sup>23</sup>H. P. Hellmeister (private communication).
- <sup>24</sup>A. Bohr and B. R. Mottelson *Nuclear Structure* (Benjamin, Reading, Mass., 1975), Vol. 2.
- <sup>25</sup>F. Dickmann and K. Dietrich, Z. Phys. **271**, 417 (1974); K. Dietrich, in *Problems of Vibrational Nuclei*, edited by G. Alaga, V. Paar, and L. Slips (North-Holland, Amsterdam, 1975), p. 333.
- <sup>26</sup>D. Janssen, R. V. Jolos, and F. Dönau, Nucl. Phys. **A224**, 93 (1974).
- <sup>27</sup>A. Arima and F. Iachello, Phys. Rev. Lett. **35**, 1069 (1975); Ann. Phys. (N.Y.) **99**, 253 (1976).
- <sup>28</sup>H. Toki and A. Faessler, Phys. Lett. **63B**, 121 (1976).
- <sup>29</sup>A. S. Davydov and G. F. Filippov, Nucl. Phys. **8**, 237 (1959); J. Meyer-ter-Vehn, Nucl. Phys. **A249**, 141 (1975).
- <sup>30</sup>A. Davydov and A. A. Chaban, Nucl. Phys. **20**, 499 (1960); A. S. Davydov and V. I. Ovcharenko, Yad. Fiz. **3**, 1011 (1966) [Sov. J. Nucl. Phys. **3**, 740 (1966)].
- <sup>31</sup>D. Proetel, *et al.*, Phys. Rev. Lett. **31**, 896 (1973); N. Rud *et al.*, *ibid.* **31**, 1421 (1973).
- <sup>32</sup>P. D. Vold, D. Cline, J. Sprinkle, and R. Scharenberg, Bull. Am. Phys. Soc. **21**, 581 (1976).
- <sup>33</sup>T. K. Das, R. M. Dreizler, and A. Klein, Phys. Rev. C **2**, 632 (1970).

<sup>34</sup>D. M. Brink, A. F. R. de Toledo-Piza, and A. K. Kerman, Phys. Lett. 19, 413 (1965).

<sup>35</sup>J. Hadermann and A. C. Rester, Nucl. Phys. A231, 120 (1974).

<sup>36</sup>A. M. Kleinfeld, A. Bockisch, and K. P. Lieb (un-

published).

<sup>37</sup>J. Barette, M. Barette, G. Lamoureux, S. Monaro, and S. Markiza, Nucl. Phys. A235, 154 (1974).

<sup>38</sup>B. Sorensen, Nucl. Phys. A177, 465 (1971).